Desalination and Water Treatment
www.deswater.com

doi: 10.1080/19443994.2015.1057530

57 (2016) 12988–12997
June

Investigation of sludge conditioning performance and mechanism by examining the effect of charge density on cationic polyacrylamide microstructure

Qingqing Guan[a,b], Mingfang Tang[a,*], Huaili Zheng[a,*], Houkai Teng[c], Xiaomin Tang[b], Yong Liao[b]

[a]*Key Laboratory of New Technology for Construction of Cities in Mountain Area, State Ministry of Education, Chongqing University, Chongqing 400045, China, Tel. +86 18716426627; email: wall-g@cqu.edu.cn (Q. Guan), Tel. +86 23 65121769; email: tmf@cqu.edu.cn (M. Tang), Tel. +86 23 65120827; email: zhl@cqu.edu.cn (H. Zheng)*
[b]*Key Laboratory of the Three Gorges Reservoir Region's Eco-Environment, State Ministry of Education, Chongqing University, Chongqing 400045, China, Tel. +86 13983828195; email: txmno1@126.com (X. Tang), Tel. +86 13452179899; email: liaoyong@cqu.edu.cn (Y. Liao)*
[c]*China National Offshore Oil Corporation (CNOOC), Tianjin Chemical Research and Design Institute, Tianjin 300131, China, Tel. +86 13602059890; email: tenghoukai@163.com*

Received 3 August 2014; Accepted 24 May 2015

ABSTRACT

The relation between the microstructure and sludge conditioning performance and mechanism of cationic polyacrylamide (CPAM) (low charge density (CD) CPAM C1, medium CD CPAM C4, and high CD CPAM C7) was extensively studied and recognized in this study. Igarashi and Pyun models based on reactivity ratio characterized the microstructure of the polymers. Results indicated that the blockness percent and mean sequence length of acrylamide (AM) unit decreased, whereas those of cationic unit increased with CD. Effect of dosage on sludge conditioning performance and mechanism was studied by measuring turbidity, filter cake moisture content (FCMC), specific resistance of filtration (SRF), floc size distribution, and zeta potential. The longest AM unit sequence length and separated cationic unit of C1 were concluded to be responsible for bridging. Moreover, the conditioning disadvantages of AM were as follows: narrow flocculation window, high optimum dosage, and maximum FCMC. On the contrary, the highest cationic blockness percent of C7 favored efficient charge neutralization, which contributed to the generation of the lowest optimum dosage. However, the SRF was significantly high, which posed as a difficulty for future treatments. The medium cationic blockness percent and mean AM unit sequence length of C4 led to the combination of charge neutralization and bridging effect with a wide flocculation window and the lowest FCMC and SRF.

Keywords: Cationic polyacrylamide; Microstructure; Sludge conditioning; Charge neutralization

---

*Corresponding authors.

1. Introduction

The increasing world-wide foundation and operation of sewage treatment plant has facilitated a better aquatic environment, but has also resulted in an important shift in waste streams from the liquid phase to the semisolid phase [1]. As activated sludge process is the most important treatment technology for a wide range of wastewaters, large amounts of waste activated sludge which represents 1 or 2% of treated waste water but contains from 50 to 80% of pollution have to be disposed of. The disposal of sewage sludge often amounts to approximately half of the total sewage treatment cost [2,3]. It has been pointed out that, dewatering step is one of the most troublesome and least understood processes of the sludge treatment. Sludge with >97% water content is highly compressible, but difficult to dewater mainly because small negatively charged particles distributed evenly in the form of a stable colloidal suspension. In order to destabilize the particulate system, chemical conditioning prior to mechanical dewatering is generally required [4–6]. Sludge conditioning, along with polyelectrolyte dosing, is a colloidal process of flocculation. In recent years, cationic polyacrylamide (CPAM) is among the most commonly used polyelectrolytes for sludge conditioning because it can neutralize the surface charge of solid particles and bridge particles through its long polymer chain to form larger flocs, which can reduce sludge-specific resistance and diminish cake compressibility [7–9].

Various features of CPAM affect the conditioning performance. Caskey and Worthington determined that the linear polymer was more effective than branched polymer of the same molecular weight (MW) in conditioning wastewater sludge [10]. Moreover, the performance of CPAM with different degrees of branching was compared in flocculating pulp suspension [11,12]. Molecular mass distributions affected flocculation efficiency [13]. Furthermore, González et al. found that blends of short- and long-chain CPAM provided complementary properties in terms of clarity of the supernatant, sedimentation rate, and compactness of the sediment compared with a single low or high MW CPAM addition [14]. The most important characteristics of CPAM that influence the efficiency of flocculation are MW and charge density (CD). MW of polyelectrolytes is directly related to the effectiveness of bridging. Zheng et al. found that polyelectrolytes with higher MW showed better conditioning effect [15]. Saveyn indicated that higher MW polyelectrolytes yield clear flocculation at low doses but tend to create elastic cakes, which cause high susceptibility to compression and limited dewaterability [16]. CD is not merely responsible for charge neutralization mechanism. CD affects the configuration of copolymer in solution as some degree of charge gives expansion of the chain on the strength of repulsion between charged segments [17]. Thus, CD determined the polyelectrolyte conformation when adsorbed on the particle surface and is therefore the predominant flocculation mechanism [18]. Zhou et al. determined that CPAM with different CD showed different mechanism [19,20]. Hjorth et al. demonstrated that the degree of charge neutralization determined flocculation mechanism [21]. In addition, Saveyn et al. found that the optimum dosage depends on the CD of polyelectrolyte [22].

The monomer unit sequence distribution of CPAM also influences the flocculation performance despite the aforementioned aspects. For instance, separately distributed or blocked cationic units greatly affect the strength between CPAM molecular chain and particle segments and further neutralization efficiency and flocculation performance [23]. However, previous research was concerned only on CD and MW rather than the microstructure. The polyelectrolyte flocculation performance and mechanism is more comprehensively understood with consideration of the microstructure. This study sheds light on the preparation study of CPAM, whose component (i.e. CD) is one of the factors that influence its microstructure. Thus, studying the effect of CD on microstructure and recognizing its relation with flocculation mechanism is important. However, no such previous research has been reported to date.

In the present study, the microstructure of CPAM with three different CDs (C1 of low CD, C4 of medium CD, and C7 of high CD) was established based on reactivity ratio. Igarashi and Pyun models depicted the microstructure of polymers. Effect of dosage on sludge conditioning performance was extensively studied through turbidity, filter cake moisture content (FCMC), SRF, floc size distribution, and zeta potential. The mechanisms of the polymers were compared and analyzed based on polymer microstructure.

2. Experimental

2.1. Materials

The monomer AM (98.5%, w/w) was obtained from Lanjie Tap Water Company (Chongqing, China). The cationic monomer acryloxyethyltrimethyl ammonium chloride (DAC) was supplied by Guangchuangjing Company (Shanghai, China). The initiator 2,2´-Azobis (2-methylpropionamide)dihydrochloride was bought from Ruihong Biological Technology (Shanghai, China).

Table 1
Characteristics of the sludge sample

Polymer	Charge density (%)	Intrinsic viscosity (ml/g)
C1	11.05	1,109
C4	40.69	1,056
C7	71.06	993

Potassium polyvinyl sulfate (PVSK) was obtained from Wako Pure Chemical Industries, Ltd. (Japan). The other reagents used in the experiments, including ethanol, urea $CO(NH_2)_2$, hydrochloric acid (HCl), and sodium hydroxide (NaOH), were of analytical grade. All aqueous and standard solutions were prepared with deionized water. The purity of nitrogen gas was higher than 99.99%.

Raw waste sludge from the thickener of Dadukou Drainage Co., Ltd. (Chongqing, China) was used for this study. The samples after collection were stored in a refrigerator maintained at 4℃ to minimize the microbial activity and analyzed within 2 d. The characteristics of the sludge are listed in Table 1.

2.2. Preparation of flocculant

CPAM was synthesized from two monomers, namely, AM and DAC, in an aqueous reaction system. AM and DAC of varying dosages were dissolved in deionized water in the reaction vessel. Urea, which acted as the cosolvent, and 2,2′-Azobis(2-methylpropionamide)dihydrochloride, which acted as the initiator, were added immediately into the aqueous solution. Meanwhile, the aqueous solution was purged with nitrogen for 30 min prior to UV activation to remove oxygen completely. Through UV-induced polymerization (main radiation wavelength: 365 nm, average irradiation intensity between 300 and 400 nm: 2,000 μW/cm^2) that continued for 1 h, the copolymer was produced and the aqueous solutions was changed into a colorless transparent solid. And then the copolymers were purified with acetone and ethanol, followed by the process, of drying and grounding into powder.

2.3. Determination of the reactivity ratio

The monomers reactivity ratios of AM with DAC were determined at low conversion (<10%). Various ratios between DAC and AM of 1:9, 2.5:7.5, 4:6, 5.5:4.5, and 7:3 were carried out. The copolymer component was from CD determination. Colloid titration was used to determine CD by Eq. (1):

$$\mathrm{CD}\ (\%) = \frac{M_{\mathrm{DAC}}C(V - V_0)}{1000\ \mathrm{m}} \times 100\% \tag{1}$$

where M_{DAC} is the relative MW of DAC, 193.67; C (mol L^{-1}) is the standard concentration of PVSK standard solution; V (mL) and V_0 (mL) are the PVSK solution titer of a sample and a blank, respectively; and m (g) is the weight of the dried sample used for titration. Reactivity ratio of AM and DAC was calculated by Kelen-Tüdös methods, which was considered more reliable than others [24].

2.4. Sludge conditioning at lab-scale

Buchner funnel test, the most common method for dewatering ability measurement, was used to investigate the conditioning ability of the polymers. The characteristics of the flocculants used in the dewatering tests were listed in Table 2. These are high MW polymers as indicated by the intrinsic viscosity [17,25,26]. Turbidity, an indication of the content of suspended particle in the liquid phase, is widely used to explain the performance of a polymer sample in various flocculation fields. Water content of sludge cake is an important aspect to be considered in the dewatering of compressible sludge. High moisture content of the filter cake is not desirable since it is responsible for large sludge volumes which increase following treatment costs. SRF is widely used to evaluate sludge filtration performance, and smaller specific resistance to filtration reflected better performance of sludge dewatering. Therefore, in this study, residual turbidity, FCMC, and SRF were used to evaluate the polymer sludge dewatering performance at various dosages. A certain dosage of flocculant (0.2%, wt) was added into 200 mL sludge at a stirring of 200 rpm for 0.5 min. After 10 min settling period, turbidity sample was collected at 1 cm below the supernatant surface (HACH 2100Q, USA). Zeta potential measurement (Zetasizer Nano ZS90, Britain) was referenced in literature [27]. And the sludge floc size distribution was measured simultaneously (BT-9300H laser particle size distribution analyzer, Dandong Bettersize Instruments Ltd., China). The conditioned sludge was poured into a Buchner funnel to filter under a vacuum pressure of 0.05 MPa for 30 min or until the vacuum could not be maintained (in <30 min). The filterability of the sludge is measured by Eq. (2):

$$\mathrm{SRF} = \frac{2bPA^2}{\mu\omega} \tag{2}$$

Table 2
Characteristics of C1, C4, and C7

Moisture content (%)	Mass density (ml/g)	pH	Zeta potential (mV)	Conductivity (mS/cm)
97.9 ± 0.15	0.967	7.04 ± 0.12	−21.6 ± 0.6	2.1 ± 0.4

where SRF is the specific resistance of the sludge (m/kg); P is the filtration pressure (N/m^2); A is the filter area (m^2); μ is the viscosity of the filtrate ($N\ s/m^2$); ω is the weight of cake solids per unit volume of filtrate (kg/m^3, $\omega = (1/C_i)/((100C_i - C_f)/100C_f)$; C_i is the initial moisture content (%); C_f is the final moisture content (%); b is the slope of filtrate discharge curve (t/V vs. V) (s/m^6), where t is the filtration time (s), and V is the volume of the filtrate [28].

FCMC (%) of the conditioned sludge was determined using Eq. (3):

$$\mathrm{FCMC} = \frac{M_T - M_f}{M_T} \tag{3}$$

where M_T is the weight of filter cake after filtration (g) and M_f is the weight of filter cake after drying at 105℃. The experiment was repeated three times and average results were reported.

3. Results and discussion

3.1. Reactivity ratio and microstructure

The monomer reactivity ratio is an important parameter of copolymerization and provides a useful tool for estimating the average compositions of copolymers and the relative placement of reactive or functional monomers along the polymer chain, i.e. the copolymer unit sequence distribution [29,30]. The copolymer compositions, as a function of feed composition, are shown in Fig. 1. Kelen-Tüdös plot determined the reactivity ratio for AM and DAC, as shown in Fig. 2. The reactivity ratio r_{AM} and r_{DAC} for the monomer pair AM and DAC, respectively, can be determined by

$$\eta = \left(r_{AM} + \frac{r_{DAC}}{\delta}\right)\xi - \frac{r_{DAC}}{\delta} \tag{4}$$

where

$$\eta = \frac{G}{H + \delta} \quad \text{and} \quad \xi = \frac{H}{H + \delta} \tag{5}$$

The transformed variables G and H are given by

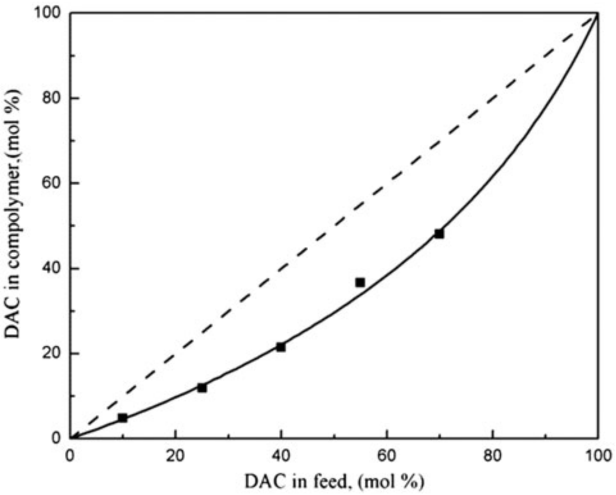

Fig. 1. Molar fraction of DAC in the copolymer (f) as a function of the molar fraction of DAC in the feed (F). (■) is for experimental results at low conversion. The solid curve represents fits with reactivity ratios calculated according to Kelen-Tüdös. The dashed line represents a copolymerization in which an ideally random copolymer would be formed.

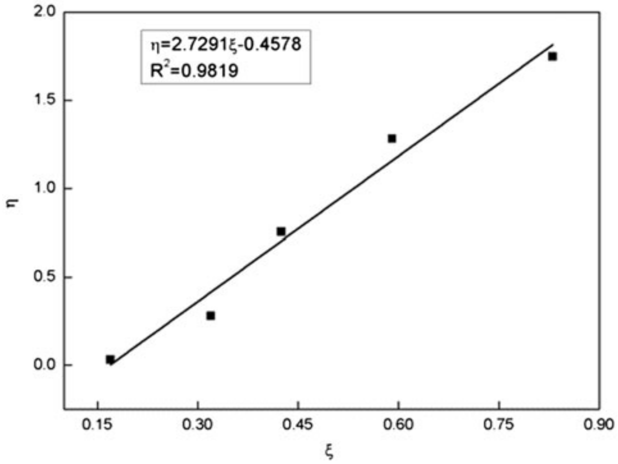

Fig. 2. Determination of reactivity ratios for copolymerization of AM with DAC by Kelen-Tüdös method.

$$G = \frac{F(f-1)}{f} \quad \text{and} \quad H = \frac{F^2}{f} \tag{6}$$

where

$f = \frac{d[\mathrm{AM}]}{d[\mathrm{DAC}]}$, copolymer instantaneous composition

$F = \frac{[\mathrm{AM}]}{[\mathrm{DAC}]}$, feed mixture instantaneous composition

The parameter δ is calculated by taking the square root of the product of the lowest and highest values of H for the copolymerization series. Reactivity ratios were determined for AM:DAC monomer pair as $r_{\mathrm{AM}} = 2.27$ and $r_{\mathrm{DAC}} = 0.38$. The graphical plot was linear, indicating that copolymerization followed the conventional copolymerization kinetics, and only the terminal monomer unit determined the reactivity of a polymer radical [31].

P(AM-co-DAC) with $r_{\mathrm{AM}}.r_{\mathrm{DAC}} = 0.86$ exhibited an opposite tendency toward alternation in this study. Moreover, the microstructures of the copolymers are expected to be important in determining the solution properties and flocculation performance of the copolymer. The reactivity ratio followed the conventional copolymerization equation, and adherence of the data to this equation is important in establishing the validity of the statistical microstructure analyses. The statistical distribution of monomer sequences DD, AA, and DA (A is for AM unit and D is for DAC unit) may be calculated by utilizing Igarashi method (7)–(9) [32,33]:

$$X = \mathrm{CD} - \frac{2\mathrm{CD}(1-\mathrm{CD})}{1+\sqrt{(2\mathrm{CD}-1)^2 + 4r_{\mathrm{AM}}r_{\mathrm{DAC}}\mathrm{CD}(1-\mathrm{CD})}} \tag{7}$$

$$Y = (1-\mathrm{CD}) - \frac{2\mathrm{CD}(1-\mathrm{CD})}{1+\sqrt{(2\mathrm{CD}-1)^2 + 4r_{\mathrm{AM}}r_{\mathrm{DAC}}\mathrm{CD}(1-\mathrm{CD})}} \tag{8}$$

$$Z = \frac{4\mathrm{CD}(1-\mathrm{CD})}{1+\sqrt{(2\mathrm{CD}-1)^2 + 4r_{\mathrm{AM}}r_{\mathrm{DAC}}\mathrm{CD}(1-\mathrm{CD})}} \tag{9}$$

where CDs the copolymer composition (i.e. CD), as shown in Table 2; and r_{AM} and r_{DAC} are the reactivity ratios for their respective monomer pairs. Mean sequence lengths μ_{AM} and μ_{DAC} are calculated through Pyun method of Eqs. (10) and (11) with consideration of reactivity ratios [24,34]:

$$\mu_{\mathrm{AM}} = 1 + r_{\mathrm{AM}}\frac{1-\mathrm{CD}}{\mathrm{CD}} \tag{10}$$

$$\mu_{\mathrm{DAC}} = 1 + r_{\mathrm{DAC}}\frac{\mathrm{CD}}{1-\mathrm{CD}} \tag{11}$$

Table 3 shows the microstructural data of the polymers based on Igarashi and Pyun model. The block structure mole percent of AM units decreased with the increase of CD. Correspondingly, μ_{AM} greatly declined. Meanwhile, the blockness molar percentage of cationic units increased from 0.89 to 48.36% with CD from 11.05 to 71.06%. However, the increasing magnitude of μ_{DAC} was not evident because of higher r_{AM} and lower r_{DAC}, which decreased the possibilities of long continuous cationic units and increased the alteration during chain growth even when the feed ratio of DAC was high. The high alteration percentage of C4 and C7 is found in Table 3.

3.2. Sludge dewatering performance and mechanism

3.2.1. Effect of dosage on dewatering performance

The effect of any flocculant on the flocculation process is influenced by the dosages; the flocculation efficiency decreases at lower or higher dosages than the optimum dose. Fig. 3 shows the effect of a flocculant dosage on residual turbidity of supernatant. Clear solid–liquid separation was not observed until the dosage was higher than 20 mg/L for C7 and 40 mg/L for C1. According to Fig. 3, residual turbidity of C7 showed a continuous increasing trend in the dosage range. By contrast, a sharp downtrend of residual turbidity with increasing polycation dose was evidenced, reaching a minimum, and then gradually increased for C1 and C4. The optimum dosage, where the lowest turbidity was achieved, was 50, 35, and 20 mg/L for C1, C4, and C7, respectively.

Table 3
Microstructural data of the polymers

Polymers	Blockness[†] (mole %)		Alteration[†] (mole %)	Mean sequence length	
	AA[††]	DD[††]	AD or DA[††]	μ_{AM}	μ_{DAC}
C1	80.89	0.89	18.23	21.43	1.04
C4	35.15	15.15	49.70	4.41	1.25
C7	8.36	48.36	43.29	1.97	1.89

[†] Statistically calculated from the reactivity ratios.

[††] A is for AM unit and D is for DAC unit.

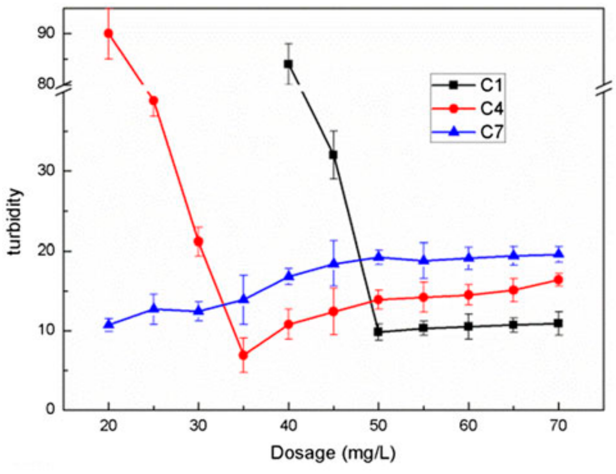

Fig. 3. Effect of dosage on residual turbidity of supernatant.

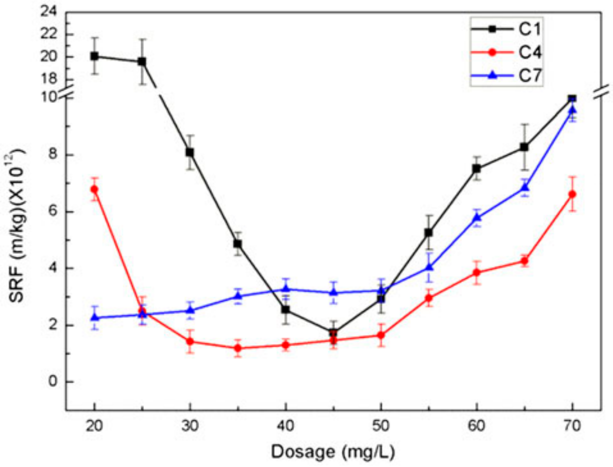

Fig. 5. Effect of dosage on SRF.

The effect of dosage on FCMC is shown in Fig. 4. FCMC, an indicator of conditioned sludge compressibility, showed an identical optimum dosage and constantly increasing tendency with turbidity of C7 [27]. However, the FCMCs of C1 and C4 were different in terms of turbidity behavior. First, the FCMC reduction stage of C1 and C4 was not as sharp as turbidity. Second, FCMC of C1 was always higher than that of C4 or C7 in most dosages. Third, C1 with an optimum dosage of 45 mg/L and C4 with broadening of the flocculation window (i.e. the optimum polymer dose range) of 30–50 mg/L were observed according to Fig. 4. The different requirements of clear supernatant and low FCMC are the reason for the inconformity. Efficient doses of polyelectrolytes and the formation of large flocs were enough to obtain clear supernatant. Nevertheless, large flocs, floc size distribution, and floc compactness were responsible for low FCMC. Moreover, FCMC of C1 was higher than those of C4 or C7 at their optimum doses, and sludge conditioned by the latter two was almost equally compressive. C7 remained the best in performance with low FCMC at the lowest optimum dosage, and no obvious restabilization occurred at overdoses such as 25–35 mg/L.

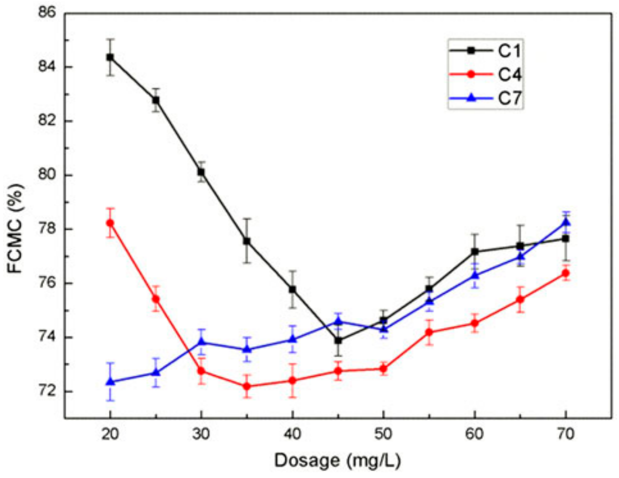

Fig. 4. Effect of dosage on FCMC.

Fig. 5 shows the effect of polymer dosage on SRF. The curved shape of SRF was similar to that of FCMC of the three polyelectrolytes. Moreover, the lowest SRF dosage or dosage range was similar with the optimum dosages of FCMC. Commonly, the goal of conditioning included both the reduction of specific resistance and the diminution of cake compressibility [35]. Therefore, the optimum dosage of C1 with 45 mg/L, C4 with 30–50 mg/L, and C7 with 20 mg/L concluded from FCMC and SRF rather than from turbidity was a more reasonable choice in this study. Nevertheless, CD and optimum dosages correlated reversely even when considering FCMC or SRF. Besides, SRF of C7 remained constant from 20 to 50 mg/L with higher SRF than that of C1 and C4 at optimum dosages. Fig. 6 shows floc size distribution at dosage of 45 mg/L for C1, C4, and C7. Previous studies found that the enlargement of floc size was thought to have produced a positive effect on dewaterability improvement [15]. The smaller floc size of C7 contributed to higher SRF. In addition, floc size of C4 was a little higher than that of C1.

3.2.2. Conditioning mechanism analysis based on polymer sequence distribution

There are two widely accepted flocculation mechanisms of sludge conditioning: particle–particle

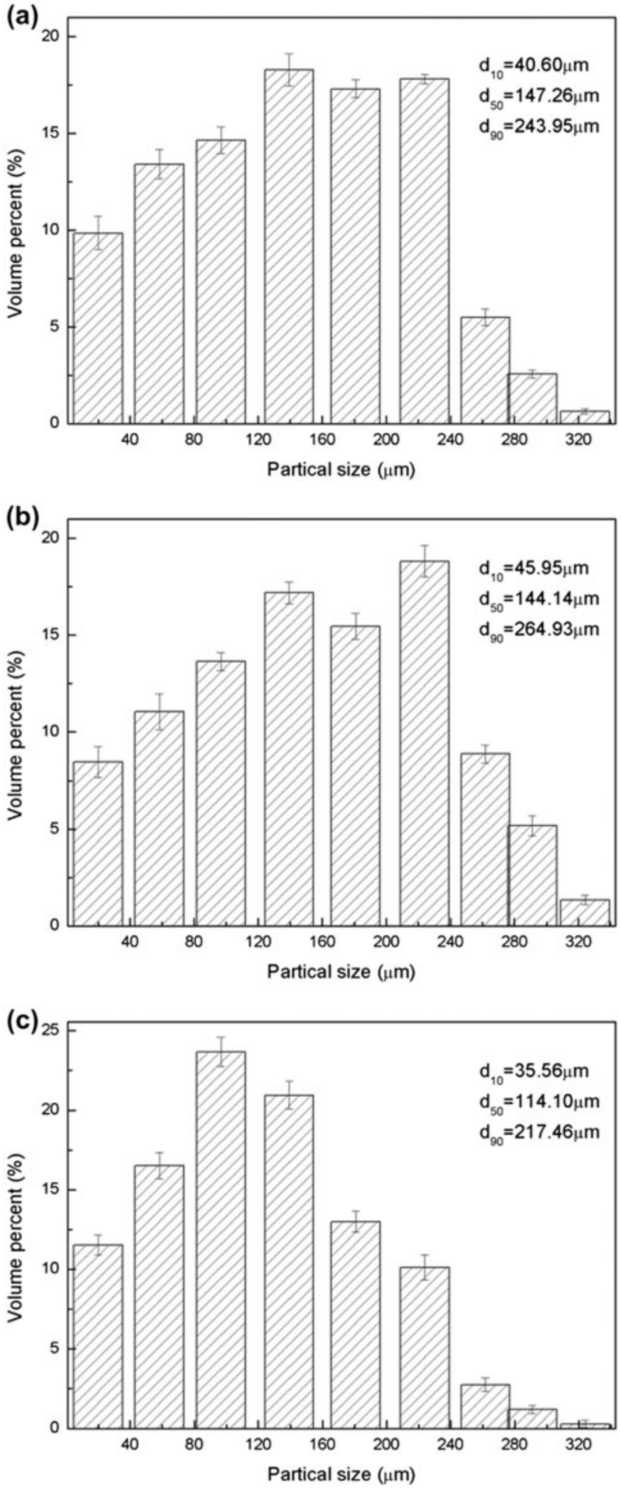

Fig. 6. Floc size distribution at dosage of 45 mg/L for (a) C1, (b) C4, and (c) C7.

bridging and surface charge neutralization [36]. Zeta potential (ζ) plays an important role in understanding charge interactions between polyelectrolyte and oppositely charged particles. Charge neutralization is the main mechanism when the most favorable flocculation performance occurs at flocculant dosages, where ζ is zero or close to zero. Repulsive forces between suspended charged particles almost diminish, and efficient flocculation occurs, which leads to effective solid–liquid separation and clear supernatant. Fig. 7 shows the effect of polyelectrolyte dosage on ζ. ζ was significantly improved after polyelectrolyte conditioning, especially in the case of C4 and C7. ζ reached zero at dosages (dose$_{\zeta=0}$) of 20.7, 34.4, and 56.5 mg/L for C1, C4, and C7, respectively, according to Fig. 7. Evidently, charge neutralization performance followed the same order with CD. In addition, the lowest residual turbidity of C4 and C7 occurred at dosages near dose$_{\zeta=0}$. The optimum dosages obtained from SRF and FCMC were also close to dose$_{\zeta=0}$ for C7. Thus, Figs. 3–6 have provided constructive evidence that charge neutralization was the main mechanism of C7 and played an important role in C4 conditioning. However, the dominant mechanism of C1 was the bridging effect. On the one hand, polymers with high MW (up to several millions) are inclined to have a flocculation mechanism of bridging based on previous studies [18]. On the other hand, the optimal dosage of C1 was 45 mg/L, which was different from dose$_{\zeta=0}$. Notably, ζ of C1 increased to −4.2 mv at optimum dosage. Charge neutralization in the case of C1 also plays a role in flocculating negatively charged particles when considering the original sludge ζ of −21.6 mV. Therefore, the mechanism of charge neutralization contributed much to efficient flocculation, considering the polyelectrolytes' optimum dosages and the corresponding dewatering performance.

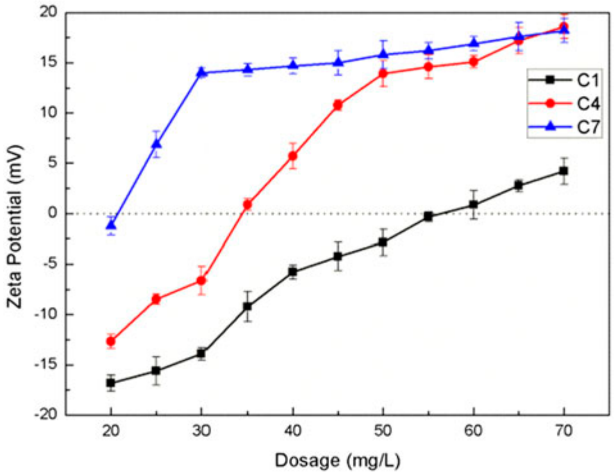

Fig. 7. Effect of dosage on zeta potential.

Thus, analyzing neutralization characteristics more comprehensively is significant.

Many studies, including the present one, indicated that polyelectrolytes with higher CD performed better in charge neutralization because they provide more cations at a specific dosage. However, $dose_{\zeta=0}$cannot reflect the cation functioning efficiency or show whether the cations are fully utilized to neutralize negative sites. Studying the cation functioning efficiency is of significance as the cationic monomer price is often the decisive factor of CPAM cost. A higher cation functioning efficiency decreases polyelectrolyte doses, which further decreases the polyelectrolyte cost. This study is the first to propose the charge neutralization index (CNI), and used it to evaluate the polymer neutralization efficiency. Here, CNI (meq/L) is the cation content that needs to bring the ζ of 1 L colloid suspension to zero and is calculated through Eq. (12):

$$\mathrm{CNI} = q \cdot \mathrm{dose}_{\zeta=0} \cdot n \tag{12}$$

$$q = 1/\left(M_{\mathrm{DAC}} + M_{\mathrm{AM}} \times \frac{1-\mathrm{CD}}{\mathrm{CD}}\right) \tag{13}$$

where q (meq/mg) is the charge content of each polymer and is calculated through Eq. (13), in which M_{AM} is the molar mass of AM (i.e. 71.08), CD is the CD of each polymer, $dose_{\zeta=0}$ is the dosage where ζ reaches zero (mg/L), and n is the cation number of one cationic unit. The CNI effectively reflects the actual charge neutralization ability of polyelectrolytes because the effect of polymer charge was eliminated by multiplying $dose_{\zeta=0}$. Clearly, a lower CNI indicates better neutralization capability because the polyelectrolyte efficaciously neutralizes negatively charged sites with lower cation supply, which means higher cation utilization efficiency. CNI of C1, C4, and C7 were 0.072, 0.116, and 0.093 meq/L, respectively, according to Eq. (12). CNI was found to be the lowest in C1, but its values in C4 were the highest. The microstructures behind CD and flocculation mechanism were accountable for the results. Nevertheless, the occurrence reason for bridging effect or charge neutralization of a specific kind of polyelectrolyte was questionable, which is explained by the polyelectrolyte sequence distribution.

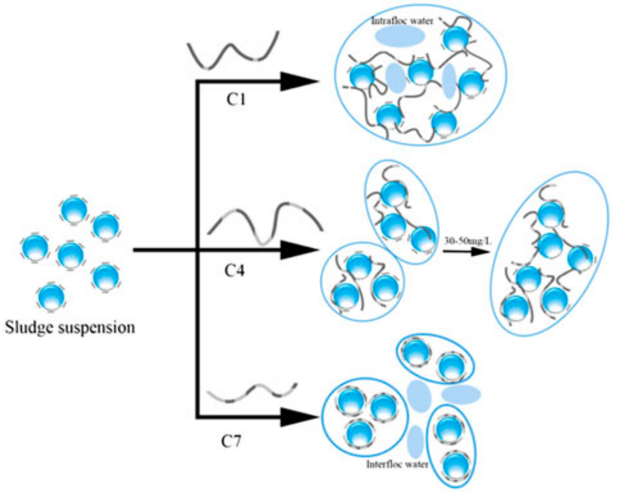

Fig. 8. Sludge conditioning mechanism diagrams of C1, C4, and C7.

A diagram illustrating the polyelectrolyte conditioning mechanism based on polymer microstructure is shown in Fig. 8. The microstructure that was calculated by reactivity ratio indicated that the cationic blockness percent of C1 was the lowest. Almost all cationic monomer units were not immediately connected with each other. Therefore, the electrostatic force between the single cationic unit and negatively segments was weak, and some of the attached points might detach again. Thus, charge neutralization, which is considered the dominant mechanism, is impossible. Contrarily, the blockness percent of the AM unit of C1 was the highest, and the mean sequence length of the AM unit was the longest according to Table 3. The structure facilitated bridging effect with the formation of loops, tails, and trains [17]. Consequently, large and loose flocs with high content of intrafloc water (water from within the floc, comprised in the loops and tails), which was not easily removed during filtration, were formed [37]. These flocs were the reason that FCMC of C1 was the highest. However, the illustration of the flocculation process was not consistent with the lowest CNI of C1 because bridging effect could lead to a positive ζ [16]. Therefore, CNI was not applicable for evaluating bridging dominated flocculation.

On the contrary, C7, with the highest cationic blockness percent, was adsorbed firmly on the negatively charged particles with strong electrostatic force. Thus, detachment was less likely to occur compared with the case of C1. Moreover, most negatively charged segments were neutralized because polyelectrolyte of high CD tended to adsorb in a rather flat equilibrium configuration, without extensive loops and tails [17]. Thus, charge neutralization was reasonable to dominate the flocculation process. The higher cationic blockness percent was the real reason of the lower CNI and optimum dosage than those of C4. Besides, the formed flocs by charge neutralization were structured by lower content intrafloc water but higher content interfloc water (water from the large voids between flocs) [16,37]. Consequently, sludge cakes with lower FCMC than that of C1 were acquired. However, the cloth filter would be more easily clogged due to its small size, as shown in Fig. 7. Moreover, weak flocs would hinder the filtration, as indicated by the relatively higher SRF, thus posing difficulty in further treatment [26,38].

The most notable phenomenon of C4 was the width of flocculation window. C4 had a medium cationic blockness percent and AM unit length, as shown in Table 3. Charge neutralization and bridging were involved in conditioning the colloid sludge system according to the deduction of C1 and C7 flocculation mechanism and the above experimental results. Polyelectrolytes cannot completely neutralize all the negatively charged sites [39]. Thus, the sludge particles were not entirely neutralized, even when positive ζ was observed. Therefore, negative segments, even C4, were added higher than $\text{dose}_{\zeta=0}$ (i.e. 50 mg/L). During such, the rearrangement of both bridging effect, the reaction between the negatively charged sites, and the non-functioning cations contributed to efficient flocculation [40]. Consequently, lower FCMC and SRF than that of C1 and C7 were observed, which facilitated the conditioning process. Moreover, the bridging effect played a role in the case of C7 conditioning at overdose. Overdose was likely to occur for high MW polymers. FCMC and SRF were not greatly increased at overdoses because a combination of bridging and charge neutralization contributes to the relative stable conditioning effect, similar with C4. Under a similar high MW, the remaining cations and negative sites resulted in rearrangement flocculation, such as that of C4.

4. Conclusion

Effect of CD on microstructure of CPAM was studied. The reactivity ratio of AM and DAC monomer pair was 2.27 and 0.38, respectively. Igarashi and Pyun models calculated through reactivity ratio indicated that blockness percent and mean sequence length of AM unit decreased, whereas those of DAC increased with CD rise.

Sludge conditioning performance and mechanism of the polymers were compared and analyzed in detail. CNI was proposed and used to evaluate polyelectrolyte cation functioning efficiency. C1 was predominated by bridging in conditioning because of its longest AM unit sequence length and separated cationic unit. The disadvantages of C1 conditioning performance were narrow flocculation window, high optimum dosage, and maximum FCMC. On the contrary, the highest cationic blockness percent of C7 favored efficient charge neutralization, which contributed to the generation of the lowest optimum dosage. However, its SRF was significantly higher, which posed difficulty for further treatment. The medium cationic blockness percent and mean AM unit length of C4 led to the combination of charge neutralization and bridging effect with a wide flocculation window, and the lowest FCMC and SRF were observed.

Acknowledgments

The authors are grateful for the financial support provided by the National Natural Science Foundation of China (Projects 21477010, 21177164).

References

[1] S. Bayar, Y. Yildiz, A. Yilmaz, A.S. Koparal, The effect of initial pH on treatment of poultry slaughterhouse wastewater by electrocoagulation method, Desalin. Water Treat. 52 (2014) 3047–3053.

[2] H. Saveyn, D. Curvers, O. Thas, P. Van der Meeren, Optimization of sewage sludge conditioning and pressure dewatering by statistical modelling, Water Res. 42 (2008) 1061–1074.

[3] J. Boráň, L. Houdková, T. Elsäßer, Processing of sewage sludge: Dependence of sludge dewatering efficiency on amount of flocculant, Resour. Conserv. Recycl. 54 (2010) 278–282.

[4] T.P. Nguyen, N. Hilal, N.P. Hankins, J.T. Novak, Characterization of synthetic and activated sludge and conditioning with cationic polyelectrolytes, Desalination 227 (2008) 103–110.

[5] M. Ma, S. Zhu, Grafting polyelectrolytes onto polyacrylamide for flocculation 2. Model suspension flocculation and sludge dewatering, Colloid Polym. Sci. 277 (1999) 123–129.

[6] P. Wolski, I. Zawieja, Hybrid conditioning before anaerobic digestion for the improvement of sewage sludge dewatering, Desalin. Water Treat. 52 (2014) 3725–3731.

[7] J. Zhu, H. Zheng, Z. Jiang, Z. Zhang, L. Liu, Y. Sun, T. Tshukudu, Synthesis and characterization of a dewatering reagent: Cationic polyacrylamide (P(AM–DMC–DAC)) for activated sludge dewatering treatment, Desalin. Water Treat. 51 (2013) 2791–2801.

[8] H. Zheng, Y. Sun, C. Zhu, J. Guo, C. Zhao, Y. Liao, Q. Guan, UV-initiated polymerization of hydrophobically associating cationic flocculants: Synthesis, characterization, and dewatering properties, Chem. Eng. J. 234 (2013) 318–326.

[9] H. Zheng, Y. Liao, M. Zheng, C. Zhu, F. Ji, J. Ma, W. Fan, Photoinitiated polymerization of cationic acrylamide in aqueous solution: Synthesis, characterization, and sludge dewatering performance, Sci. World J. 2014 (2014) 1–11.

[10] J.A. Caskey, D. Worthington, Tailoring Flocculant Molecular Structure to Improve the Conditioning and Dewatering of Wastewater Sludges, Water Resources Research Center, Purdue University, Lafayette, IN, 1987.

[11] Á. Blanco, E. Fuente, M.C. Monte, N. Cortés, C. Negro, Polymeric branched flocculant effect on the flocculation process of pulp suspensions in the papermaking industry, Ind. Eng. Chem. Res. 48 (2009) 4826–4836.

[12] E. Antunes, F.A.P. Garcia, P. Ferreira, A. Blanco, C. Negro, M.G. Rasteiro, Effect of water cationic content on flocculation, flocs resistance and reflocculation capacity of PCC induced by polyelectrolytes, Ind. Eng. Chem. Res. 47 (2008) 6006–6013.

[13] S.K. Dentel, M.M. Abu-Orf, C.A. Walker, Optimization of slurry flocculation and dewatering based on electrokinetic and rheological phenomena, Chem. Eng. J. 80 (2000) 65–72.

[14] G. González, J.C. de la Cal, J.M. Asua, Flocculation efficiency of blends of short and long chain polyelectrolytes, Colloids Surf., A 385 (2011) 166–170.

[15] H. Zheng, Y. Sun, J. Guo, F. Li, W. Fan, Y. Liao, Q. Guan, Characterization and evaluation of dewatering properties of PADB, a highly efficient cationic flocculant, Ind. Eng. Chem. Res. 53 (2014) 2572–2582.

[16] H. Saveyn, S. Meersseman, O. Thas, P. Van der Meeren, Influence of polyelectrolyte characteristics on pressure-driven activated sludge dewatering, Colloids Surf., A 262 (2005) 40–51.

[17] B. Bolto, J. Gregory, Organic polyelectrolytes in water treatment, Water Res. 41 (2007) 2301–2324.

[18] M.G. Rasteiro, F.A.P. Garcia, P. Ferreira, A. Blanco, C. Negro, E. Antunes, The use of LDS as a tool to evaluate flocculation mechanisms, Chem. Eng. Process. 47 (2008) 1329–1338.

[19] Y. Zhou, G.V. Franks, Flocculation mechanism induced by cationic polymers investigated by light scattering, Langmuir 22 (2006) 6775–6786.

[20] Y. Zhou, G.J. Jameson, G.V. Franks, Influence of polymer charge on the compressive yield stress of silica aggregated with adsorbed cationic polymers, Colloids Surf., A 331 (2008) 183–194.

[21] M. Hjorth, B.U. Jørgensen, Polymer flocculation mechanism in animal slurry established by charge neutralization, Water Res. 46 (2012) 1045–1051.

[22] H. Saveyn, D. Curvers, R. Dupont, P. Van der Meeren, Determination of charge density and adsorption behaviour of DMAEA-Q-based cationic polymers by fluorimetric analysis, Water Res. 43 (2009) 1905–1912.

[23] M. Ma, S. Zhu, Grafting polyelectrolytes onto polyacrylamide for flocculation 1. Polymer synthesis and characterization, Colloid Polym. Sci. 277 (1999) 115–122.

[24] P. Bera, S.K. Saha, Water-soluble copolymers of acrylamide with diacetone-acrylamide and N-t-butylacrylamide on aqueous montmorillonite surface: Synthesis and characterisation, Eur. Polym. J. 36 (2000) 411–419.

[25] E. Arinaitwe, M. Pawlik, A role of flocculant chain flexibility in flocculation of fine quartz. Part I. Intrinsic viscosities of polyacrylamide-based flocculants, Int. J. Miner. Process. 124 (2013) 50–57.

[26] S.R. Gray, C.B. Ritchie, Effect of organic polyelectrolyte characteristics on floc strength, Colloids Surf., A 273 (2006) 184–188.

[27] K.B. Thapa, Y. Qi, A.F.A. Hoadley, Interaction of polyelectrolyte with digested sewage sludge and lignite in sludge dewatering, Colloids Surf., A 334 (2009) 66–73.

[28] J.P. Wang, S.J. Yuan, Y. Wang, H.Q. Yu, Synthesis, characterization and application of a novel starch-based flocculant with high flocculation and dewatering properties, Water Res. 47 (2013) 2643–2648.

[29] X. Wang, Q. Yue, B. Gao, X. Si, X. Sun, S. Zhang, Kinetics of dispersion polymerization of dimethyl diallyl ammonium chloride and acrylamide, J. Polym. Res. 18 (2010) 1067–1072.

[30] M.R. Aguilar, A. Gallardo, M.d.M. Fernández, J.S. Román, In Situ quantitative ^{1}H NMR monitoring of monomer consumption: A simple and fast way of estimating reactivity ratios, Macromolecules 35 (2002) 2036–2041.

[31] S. Iwatsuki, A. Kondo, H. Harashina, Free radical copolymerization behavior of methyl α-(trifluoromethyl)acrylate and α-(trifluoromethyl)acrylonitrile: Penultimate monomer unit effect and monomer reactivity parameters, Macromolecules 17 (1984) 2473–2479.

[32] D.-J. Liaw, C.-C. Huang, H.-C. Sang, P.-L. Wu, Macromolecular microstructure, reactivity ratio and viscometric studies of water-soluble cationic and/or zwitterionic copolymers, Polymer 41 (2000) 6123–6131.

[33] S. Igarashi, Representation of composition and blockiness of the copolymer by a triangular coordinate system, J. Polym. Sci., Part C: Polym. Lett. 1 (1963) 359–363.

[34] C.W. Pyun, Comonomer and stereosequence distributions in high polymers, J. Polym. Sci. Part A2: Polym. Phys. 7 (1970) 1111–1126.

[35] Y.Q. Zhao, D.H. Bache, Conditioning of alum sludge with polymer and gypsum, Colloids Surf., A 194 (2001) 213–220.

[36] D. Ghernaout, B. Ghernaout, Sweep flocculation as a second form of charge neutralisation—A review, Desalin. Water Treat. 44 (2012) 15–28.

[37] J. Vaxelaire, J. Olivier, Conditioning for municipal sludge dewatering. From filtration compression cell tests to belt press, Drying Technol. 24 (2006) 1225–1233.

[38] T. Li, Z. Zhu, D. Wang, C. Yao, H. Tang, Characterization of floc size, strength and structure under various coagulation mechanisms, Powder Technol. 168 (2006) 104–110.

[39] Y.-K. Leong, J. Teo, E. Teh, J. Smith, J. Widjaja, J.-X. Lee, A. Fourie, M. Fahey, R. Chen, Controlling attractive interparticle forces via small anionic and cationic additives in kaolin clay slurries, Chem. Eng. Res. Des. 90 (2012) 658–666.

[40] J. Yu, D. Wang, X. Ge, M. Yan, M. Yang, Flocculation of kaolin particles by two typical polyelectrolytes: A comparative study on the kinetics and floc structures, Colloids Surf., A 290 (2006) 288–294.